

# PRELIMINARY GEOMETRY OPTIMIZATION OF A 3.5-CELL SRF GUN CAVITY AT ELBE BASED ON BEAM DYNAMICS \*

K. Zhou, Institute of Applied Electronics, CAEP, Mianyang, China  
Institute of Radiation Physics, HZDR, Dresden, Germany  
P. Li, Institute of Applied Electronics, CAEP, Mianyang, China  
A. Arnold, J. Schaber, J. Teichert<sup>†</sup>, R. Xiang, S. Ma  
Institute of Radiation Physics, HZDR, Dresden, Germany

## Abstract

At present, ELBE radiation source at HZDR is optimizing the SRF cavity for the next generation ELBE SRF GUN. This paper presents a preliminary study on the geometry optimization of a 3.5-cell SRF gun cavity based on beam dynamics. By changing the lengths of the half cell and the first TESLA like cell, two new cavity models with higher electric field in the half cell are built and their RF fields are compared with SRF GUN I and SRF GUN II. Through the scanning of the RF phases and the electric fields, the simulation results indicate that new models have smaller transverse emittance at relatively lower electric field gradients and better performance on longitudinal emittance than SRF GUN I and SRF GUN II.

## INTRODUCTION

Developing electron sources delivering high quality electron beams is always an active research field for high intensity particle accelerators, such as free electron laser (FEL), energy recovery linacs (ERLs) and electron linear colliders. Superconducting radio-frequency electron gun (SRF gun) is a superior alternative, which is capable to generate high-brightness and low-emittance electron beams when operating in continuous wave (CW) mode. The concept of SRF gun was firstly proposed in 1988 [1], and the first experiments were carried out at the University of Wuppertal four years later [2]. In 2002, world's first electron beams were obtained by the Drossel SRF gun at FZD (now HZDR) [3]. Inspired by this success, SRF gun projects based on different approaches were launched worldwide [4].

In 2004, a SRF photoelectron injector (SRF GUN I) was developed at HZDR in collaboration with DESY, HZB and MBI [5], as shown in Fig. 1. SRF GUN I was the world's first SRF gun with a 3.5-cell niobium cavity operating for a linac and was used to demonstrate the first lasing with the far-infrared FEL at ELBE [6].

After the proof-of-principle demonstration of SRF GUN I, an improved SRF gun (SRF GUN II) was developed as shown in Fig. 2 and has been in operation up to now. Comparing to SRF GUN I, the electric field strength in the first half cell was improved, and a superconducting solenoid was installed in the cryomodule [7]. The influences of RF focus,

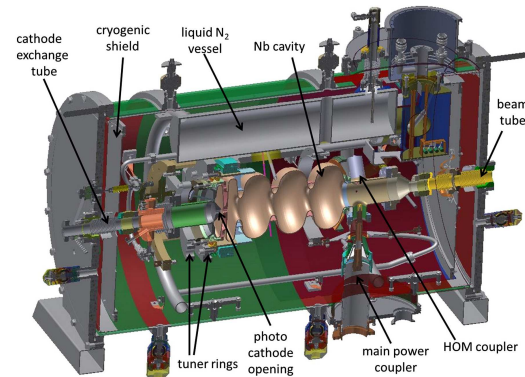


Figure 1: ELBE SRF GUN I.

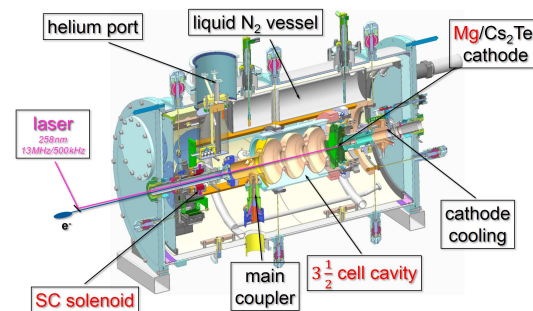


Figure 2: ELBE SRF GUN II.

cathode position and superconducting solenoid on emittance compensation have been investigated in detail [8].

Due to a degradation of available maximum field gradient of SRF GUN II, the construction of the third version, SRF GUN III, was initiated with the same niobium cavity of SRF GUN I refurbished at DESY and a newly built cryomodule with a superconducting solenoid [9].

At present, HZDR is also optimizing the SRF cavity for the next generation ELBE SRF GUN. To optimize the geometry of the 3.5-cell SRF gun cavity, the distributions of the electromagnetic fields and output beam qualities with different geometric models have been investigated and compared [10]. This paper mainly presents an analysis of the output beam parameters of two new models comparing to SRF GUN I and SRF GUN II.

\* Work supported by National Natural Science Foundation of China with Grant [11605190 and 11805192].

<sup>†</sup> Email address: j.teichert@hzdr.de

Table 1: Geometry Changes of New Models Comparing to SRF GUN I and SRF GUN II (unit:mm)

Models	SRF GUN I	SRF GUN II	New Model I	New Model II
Z1	25	25.6	25.8	26
Z2	51.89	51.3	51.0	50.8

Table 2: Physical Parameters of New Models Comparing to SRF GUN I and SRF GUN II

Models	Freq. (MHz)	$E_{peak1}/E_{peak}$	$E_{max}/E_0$	$B_{max}/E_0$ mT/(MV/m)	Field Flatness	r/Q
SRF GUN I	1297.67693	64.5%	2.174	4.285	97.8%	336.8
SRF GUN II	1297.66094	81.5%	2.661	5.060	99.0%	330.5
New Model I	1297.62255	88.0%	2.848	5.353	98.8%	327.3
New Model II	1297.67210	97.1%	3.104	5.771	99.1%	323.0

## NEW MODELS

The geometry differences between SRF GUN I and SRF GUN II are only located at the first half cell and the first TESLA like cell as shown in Fig. 3. Z1 refers to the length of the right part of the first half cell and Z2 represents the length of the left part of the first TESLA like cell. By appropriately increasing Z1 and decreasing Z2, the electric field gradient in the first half cell can be improved significantly, without changing the electric fields in the TESLA like cells.

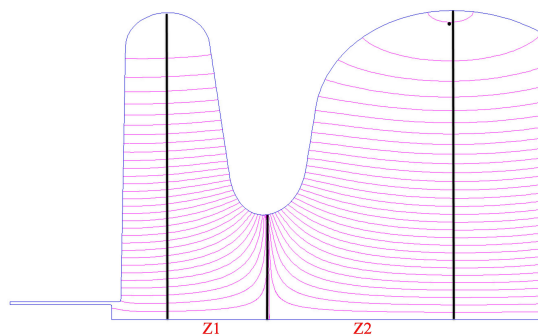


Figure 3: The changing areas of the cavity models.

In this paper, two new cavity models have been built by changing the length of Z1 and Z2 as shown in Table. 1. Figure 4 shows their absolute electric fields on axis normalized to  $E_{peak} = 50$  MV/m, where  $E_{peak}$  refers to the maximum value of electric field along the central axis. The major differences of their RF fields are located in the half cell. Their physical parameters calculated with Superfish are listed in Table 2, in which  $E_0$  is the average electric field gradient along the central axis;  $E_{peak1}$  is the maximum electric field gradient in the first half cell;  $E_{max}$  is the maximum electric field of the whole cavity and  $B_{max}$  is the maximum magnetic field of the whole cavity. The resonant frequency and field flatness almost remain unchanged. Their field flatnesses are all better than 97.5%. The value of r/Q decreases a little but not much.  $E_{peak1}/E_{peak}$  of New Model I and New Model II have been improved to 88% and 97.1%, respectively. Mean-

while, both  $E_{max}/E_0$  and  $B_{max}/E_0$  of New Model I and New Model II also increase obviously.

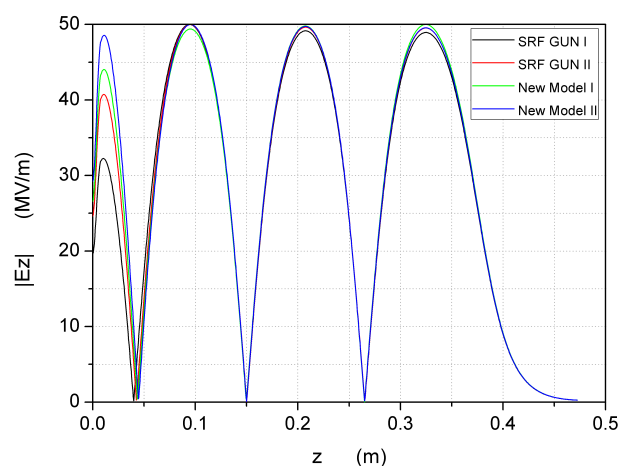


Figure 4: On-axis field profiles of these cavity models normalized to  $E_{peak} = 50$  MV/m.

## SIMULATION RESULTS

To evaluate how much influence the cavity geometry has on beam dynamics, the RF fields of these models were extracted from Superfish and imported to Astra to calculate their output beam parameters.

In order to compare independently, the simulation did not consider the bias voltage applied on the photocathode and the focus solenoid located at the downstream of the SRF cavity. The initial electron distributions at the photocathode are all the same for these four models. The bunch charge is 100 pC. The laser pulse length is 3 ps, the initial rms radius is 0.5 mm and the initial transverse emittance is 0.05 mm mrad.

Figure 5 and Figure 6 present the output transverse emittance and longitudinal emittance of these models, respectively. They are intensity graphs by scanning the RF phase from  $20^\circ$  to  $70^\circ$  and electric field  $E_{peak}$  from 20 MV/m to 50 MV/m. The color of each pixel represents the corresponding

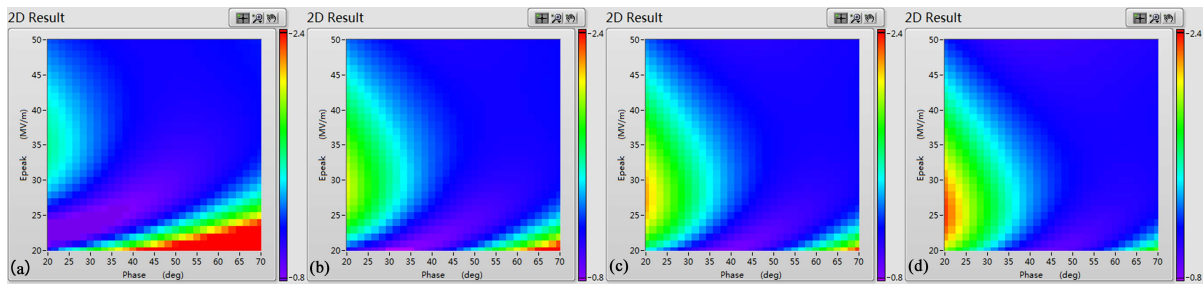


Figure 5: Output transverse emittance ( $\pi$  mm mrad) of (a) SRF GUN I, (b) SRF GUN II, (c) New Model I and (d) New Model II.

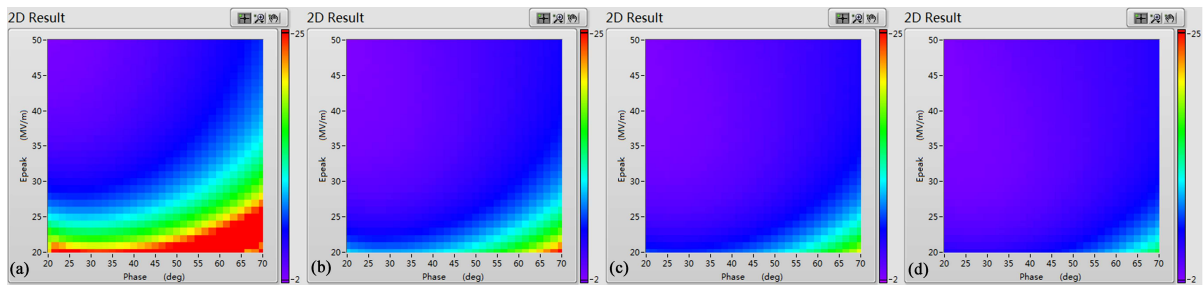


Figure 6: Output longitudinal emittance ( $\pi$  keV mm) of (a) SRF GUN I, (b) SRF GUN II, (c) New Model I and (d) New Model II.

value at the exit of the cryomodule where  $z = 1$  m from the photocathode, while the cavity length is about 0.47 m.

In Fig. 5, the variations of the transverse emittance for these four models are similar. With the increase of the electric field gradient, the RF phase corresponding to the minimum transverse emittance will also shift to a larger value. This is reasonable because the RF phase needs to be adjusted to match the electrons acceleration when traveling through the cavity cell under different electric field gradients at low energy. Another interesting variation is that the region of the minimum output transverse emittance (purple area) moves to higher RF phases and lower electric fields from SRF GUN I to New Model II. So New Model I and New Model II have better performance on transverse emittance at relatively low electric fields ( $E_{peak} < 20$  MV/m), while in high electric field regions, there are not much differences.

As for the longitudinal direction, in Fig. 6, it is obvious that the longitudinal emittance increases with the RF phase and decreases with the electric field. And New Model I and New Model II offer smaller output longitudinal emittances than SRF GUN I and SRF GUN II, especially at low electric fields.

## CONCLUSION

By changing the lengths of the half cell and the first TESLA like cell, we built two new cavity models with higher  $E_{peak1}/E_{peak}$  than SRF GUN I and SRF GUN II. Their RF fields were compared and used to calculate their output beam parameters. Through the scanning of the RF phases and the electric fields, the simulation results indicate that New Model I and New Model II have lower transverse emittance

at relatively lower electric fields and better performance on longitudinal emittance than SRF GUN I and SRF GUN II.

## ACKNOWLEDGEMENT

The authors would like to thank the SRF group of ELBE team for their great help. This work is supported by State Administration of Foreign Experts Affairs P.R.China and China Academy of Engineering Physics.

## REFERENCES

- [1] H. Chaloupka, *et al*, "A proposed superconducting photoemission source of high brightness", *Nuclear Instruments and Methods A*, 285 (1989) 327. doi:10.1016/0168-9002(89)90474-9
- [2] A. Michalke, Ph.D thesis, University of Wuppertal, 1992, WUB-DIS 92-5.
- [3] D. Janssen, *et al*, "First operation of a superconducting RF-gun", *Nuclear Instruments and Methods A*, 507, 314-317, 2003. doi:10.1016/S0168-9002(03)00936-7
- [4] A. Arnold, *et al*, "Overview on superconducting photoinjectors", *Physical Review Special Topics - Accelerators and Beams*, 14 (2011) 024801. doi:10.1103/PhysRevSTAB.14.024801
- [5] A. Arnold, *et al*, "Development of a superconducting radio frequency photoelectron injector", *Nuclear Instruments and Methods A*, 577, p.440, 2007. doi:10.1016/j.nima.2007.04.171
- [6] J. Teichert, *et al*, "Free-electron laser operation with a superconducting radio-frequency photoinjector at ELBE", *Nuclear Instruments and Methods A*, 743 (2014) 114. doi:10.1016/j.nima.2014.01.006

Content from this work may be used under the terms of the CC BY 3.0 licence (© 2019). Any distribution of this work must maintain attribution to the author(s), title of the work, publisher, and DOI

- [7] A. Arnold, *et al*, *LINAC2014*, Geneva, Switzerland, TUPP066, 578. 10.1103/PhysRevAccelBeams.21.093403
- [8] H. Vennekate, *et al*, Emittance compensation schemes for a superconducting rf injector”, *Physical Review Accelerators and Beams*, 21 (2018) 093403. doi:10.1103/PhysRevAccelBeams.21.093403
- [9] H. Vennekate, *et al*, “Building the Third SRF Gun at HZDR”, *IBIC2017*, Grand Rapids, MI, USA, MOPWC01, 98. doi :
- [10] K. Zhou, *et al*, “Geometry Dependent Beam Dynamics of a 3.5-cell SRF Gun Cavity at ELBE”, *SRF2019*, Dresden, Germany, THP082. doi :10.18429/JACoW-SRF2019-THP082

Content from this work may be used under the terms of the CC BY 3.0 licence (© 2019). Any distribution of this work must maintain attribution to the author(s), title of the work, publisher, and DOI